



UDC 621.762

<https://doi.org/10.17073/1997-308X-2024-1-31-39>Research article
Научная статья

Influence of copper on the microstructure and mechanical properties of titanium ortho-alloy produced by selective laser melting

I. A. Polozov[✉], V. V. Sokolova, A. M. Gracheva, A. A. PopovichPeter the Great St. Petersburg Polytechnic University
29 Polytekhnicheskaya Str., St. Petersburg 195251, Russian Federation polozov_ia@spbstu.ru

Abstract. This study explores an intermetallic orthorhombic titanium alloy produced by incorporating varying copper concentrations ranging from 0 to 6 wt. % through in-situ doping during selective laser melting (SLM) fabrication, coupled with simultaneous substrate preheating. The investigation delves into the influence of copper introduction on grain refinement within the primary B2/ β -phase and subsequent alterations in mechanical properties. Through *X*-ray diffraction analysis and scanning electron microscopy, the microstructure characterized by the presence of the B2/ β -phase and orthorhombic phase precipitates was identified. Additionally, the detection of a minor quantity of the α_2 -Ti₃Al-phase was noted, with its proportion increasing proportionally with the augmentation of copper content. Differential scanning calorimetry revealed a shift in the phase transformation temperatures towards higher temperatures and a constricted α_2 -Ti₃Al + B2/ β + Ti₂AlNb region, attributed to the inclusion of copper. The addition of copper, up to 6 wt. %, resulted in the softening and embrittlement of the orthorhombic alloy, forming a fine-grained microstructure with an average grain size of 8.3 μ m. Energy dispersive *X*-ray spectroscopy confirmed the presence of an intermetallic O-phase along the grain boundaries, contributing to a 12 % increase in hardness compared to the orthorhombic alloy without copper after SLM with substrate heating at 850 °C. An alloy containing 4 wt. % copper exhibited superior plastic properties and a tensile strength of 1080 MPa, comparable to the strength of the orthorhombic alloy obtained via SLM followed by hot isostatic pressing.

Keywords: orthorhombic alloy, additive manufacturing, aviation alloys, doping, *in situ* doping

Acknowledgements: The research is supported by the grant awarded by the Russian Science Foundation No. 23-79-30004, <https://rscf.ru/project/23-79-30004/>.

For citation: Polozov I.A., Sokolova V.V., Gracheva A.M., Popovich A.A. Influence of copper on the microstructure and mechanical properties of titanium ortho-alloy produced by selective laser melting. *Powder Metallurgy and Functional Coatings*. 2024; 18(1):31–39. <https://doi.org/10.17073/1997-308X-2024-1-31-39>

Влияние меди на микроструктуру и механические свойства титанового орто-сплава, изготовленного методом селективного лазерного плавления

И. А. Полозов[✉], В. В. Соколова, А. М. Грачева, А. А. Попович

Санкт-Петербургский политехнический университет Петра Великого
Россия, 195251, г. Санкт-Петербург, ул. Политехническая, 29

✉ polozov_ia@spbstu.ru

Аннотация. Проведено исследование интерметаллидного орторомбического титанового сплава, полученного методом селективного лазерного плавления (СЛП) с добавлением меди в количестве от 0 до 6 мас. % с помощью *in situ* легирования в процессе изготовления с использованием подогрева подложки от 300 до 850 °С. Показано, что введение меди в сплав способствовало измельчению зерна первичной В2/β-фазы и изменению механических свойств. В результате рентгеноструктурного анализа и сканирующей микроскопии была выявлена микроструктура, состоящая из В2/β-фазы с выделениями орторомбической фазы. Также в образцах прослеживается наличие небольшого количества α₂-Ti₃Al-фазы, количество которой увеличивается с повышением содержания меди в сплаве. Методом дифференциальной сканирующей калометрии установлено, что добавление меди приводит к смещению температур фазовых превращений в область более высоких температур и сужает область α₂-Ti₃Al + В2/β + Ti₂AlNb. Введение меди до 6 мас. % обуславливает разупрочнение и охрупчивание орторомбического сплава с формированием мелкозернистой микроструктуры, средний размер зерна которой составил 8,3 мкм. Результаты энергодисперсионной рентгеновской спектроскопии показали наличие на границах зерен интерметаллидной О-фазы, что способствовало увеличению твердости на 12 % в сравнении с орторомбическим сплавом без добавления меди после СЛП с подогревом подложки при 850 °С. Наилучшие пластические свойства проявил сплав с содержанием меди 4 мас. % при пределе прочности 1080 МПа, что сопоставимо со значением прочности орто-сплава, полученного методом СЛП после горячего изостатического прессования.

Ключевые слова: орторомбический сплав, аддитивное производство, авиационные сплавы, легирование, *in situ* легирование

Благодарности: Исследование выполнено за счет гранта Российского научного фонда № 23-79-30004, <https://rscf.ru/project/23-79-30004/>.

Для цитирования: Полозов И.А., Соколова В.В., Грачева А.М., Попович А.А. Влияние меди на микроструктуру и механические свойства титанового орто-сплава, изготовленного методом селективного лазерного плавления. *Известия вузов. Порошковая металлургия и функциональные покрытия*. 2024;18(1):32–39. <https://doi.org/10.17073/1997-308X-2024-1-31-39>

Introduction

Titanium aluminide-based intermetallic alloys have garnered significant attention among researchers as potential heat-resistant materials to replace nickel alloys in automotive and aerospace industries. Among these, orthorhombic titanium alloys stand out due to their exceptional heat and creep resistance, attributed to the presence of the orthorhombic intermetallic Ti₂AlNb [1]. However, the existence of this intermetallic phase poses challenges in fabricating products using traditional methods [2–4].

Modern orthorhombic titanium aluminide alloys surpass previous generations based on the Ti₃Al intermetallic compound in various aspects. It is widely acknowledged that incorporating β-isomorphous dopants such as Mo, V, Ta, and especially Nb, into titanium aluminide-based alloys has enhanced their creep and strength properties at elevated temperatures [5–7]. Copper doping has been employed to combat the embrittlement of titanium alloys at lower temperatures while improving

their strength characteristics [8]. Previous studies indicate that resulting eutectics in such alloys contain the Ti₂Cu intermetallic compound, acting as a strengthening agent [9; 10]. The addition of copper also aids in reducing temperature gradients during the laser molding process in a powder bath tank, promoting the formation of equiaxed eutectoid grains in binary alloys due to the solutal undercooling effect [11; 12]. Despite copper's positive impact on enhancing thermal conductivity and heat resistance, the divergence in melting temperatures among components heightens the risk of gas pore and crack formation [13].

The intermetallic casting of titanium alloys demands strict adherence to specific fabrication conditions, including a high-quality surface for casting molds, elevated temperatures, and a protective atmosphere to prevent defect formation [14]. These alloys possess higher brittleness and reduced machinability, leading to labor-intensive and costly machining processes [15; 16]. Consequently, there is relevance in exploring additive technologies (AT) for manufacturing products from

intermetallic titanium alloys [17; 18]. the application of At in producing intermetallic alloys often leads to crack formation and involves significantly higher cooling rates compared to casting processes. This discrepancy contributes to the generation of substantial thermal stresses [13]. To mitigate thermal stress in selective laser melting (SLM) technology, controlling temperature conditions during crystallization becomes essential. Studies have demonstrated that the production of defect-free intermetallic samples necessitates additional high-temperature substrate preheating during SLM [19]. It has been observed that heating the substrate above 800 °C is necessary to achieve defect-free samples from Ti_2AlNb ortho-alloys incorporating microalloying elements [20]. Nevertheless, the influence of copper on the processability of ortho-alloy production during SLM remains insufficiently explored [21].

In situ synthesis represents a relatively new approach that holds the potential to streamline fabrication processes and reduce production costs for new alloys and their associated products. The synthesis of required composition alloys from elemental powders has conventionally been achieved through powder metallurgy methods, including techniques like hot isostatic pressing (HIP) [22] and spark plasma sintering [23]. These methods have also found application in titanium-based alloys, notably in selective laser melting and other additive manufacturing technologies [21; 24; 25].

This article presents the outcomes of an *in situ* investigation involving the doped orthorhombic titanium alloy produced via selective laser melting. The study examines structure formation and alterations in phase composition resulting from the addition of copper in quantities ranging from 0 to 6 wt. %.

Experimental

For this research, a powder mixture was employed, derived from blending ortho-alloy powder

$Ti-22Al-23Nb-0.8Mo-0.3Si-0.4C-0.1B-0.2Y$ (at. %) (manufactured by AMC Powders Co. Ltd, China) and PMS-1 copper powder in varying proportions of 2, 4, and 6 wt. % (Fig. 1). The blending process involved a vertical mixer and lasted for 12 h. The copper powder, with a purity level of 99.5 %, was manufactured via the electrolyte method and characterized by dendritic particle morphology. The initial powder of the ortho-alloy consisted of spherical particles with an average size of $d_{50} = 33 \mu m$, produced through the gas atomization method.

Samples measuring $10 \times 10 \times 10$ mm were manufactured for microstructure analysis from the prepared mixture using the SLM method on AconityMIDI unit (Aconity3D GmbH, Germany). fitted with a fiber laser with a wavelength of 1070 nm and a maximum power of 1000 W. The samples were fabricated in a protective argon atmosphere, and the substrate was preheated to temperatures of 300, 500, and 850 °C prior to the commencement of laser processing. The chosen range of substrate preheating temperatures aligned with the region of the eutectoid transformation of Ti_2Cu , as well as based on insights gleaned from previous studies on SLM processes involving orthorhombic alloys [26].

During the SLM method, samples were fabricated using a volumetric energy density level set at $49 J/mm^3$. Selection of the primary process parameters for SLM was based on prior investigations into the SLM process for the ortho-alloy [20], ensuring conditions that would yield samples with a relative density exceeding 99 %. Samples with a diameter of 12 mm and a length of 70 mm were produced for the examination of mechanical properties. These samples were further machined to comply with the sizes specified by GOST 1497-84.

Microstructural and energy dispersive analyses (EDX) were conducted using a Mira 3 LMU scanning electron microscope (Tescan, Czech Republic). X-ray phase analysis (XPA) was performed employing a Bruker D8 Advance X-ray diffractometer (Bruker,

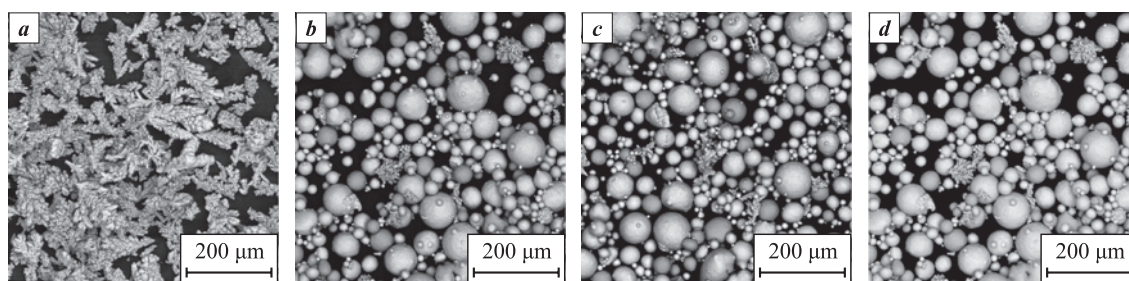


Fig. 1. SEM images of initial copper powder (a) and powder mixture ortho-alloy + copper at various Cu contents (b–d)

Cu, wt. %: b – 2; c – 4; d – 6

Рис. 1. СЭМ-изображения исходного порошка меди (a) и порошковой смеси орто-сплав + медь при различном содержании меди (b–d)

Cu, мас. %: b – 2; c – 4; d – 6

Bremen, Germany) using CuK_α radiation ($\lambda = 1.5418 \text{ \AA}$). Differential scanning calorimetry (DSC) was carried out using a STA409 Netzch/Pegasus analyzer (Netzch, Germany) employing a heating rate of $10 \text{ }^\circ\text{C/min}$ in an argon flow environment. Hardness measurements of the samples were taken using a Buehler VH1150 unit (Buehler, USA) under a 500 g load. Tensile tests were conducted on a Zwick/Roell Z100 testing machine (Zwick/Roell, Germany).

Results and discussion

Fig. 2 displays images showcasing microstructures of ortho-alloy with 6 wt. % copper, produced using the SLM method at different substrate preheating temperatures. The microstructure and phase composition of the ortho-alloy, when combined with copper, exhibit considerable changes based on alterations in the substrate temperature during the SLM process. At a relatively low preheating temperature of $300 \text{ }^\circ\text{C}$, the microstructure manifests as a single-phase structure comprising the $\text{B2}/\beta$ phase with a bcc lattice (Fig. 2, *a*). Notably, thermal stress-induced cracks are observed on these samples. Elevating the preheating temperature to $500 \text{ }^\circ\text{C}$ induces the precipitation of the orthorhombic Ti_2AlNb -phase (dark gray color) along the boundaries of primary β -grains (Fig. 2, *b*). Further escalation of the temperature to $850 \text{ }^\circ\text{C}$ initiates the thickening of ortho-phase precipitates along β -grain boundaries (Fig. 2, *c*). Additionally, finely dispersed needle-shaped ortho-phase precipitates (gray color) begin to form within the β -grains. Notably, regions with higher copper content were not detected through microstructural analysis. Energy dispersive analysis confirmed the homogeneous distribution of copper throughout the sample volume post-SLM of the powder mixture.

The observed transformations in microstructure and phase composition of the ortho-alloy, coupled with copper addition, as influenced by varying substrate pre-

heating temperatures, align with previous research conducted on the ortho-alloy without copper [20]. However, the addition of copper notably facilitated the prominent formation of ortho-phase precipitates near boundaries and led to a reduction in the size of primary β -grains.

To mitigate crack defects in ortho-alloy samples combined with copper, it became evident that higher substrate preheating temperatures were necessary. At temperatures of $t = 300$ and $500 \text{ }^\circ\text{C}$, the fabricated samples exhibited cracks due to substantial residual stresses, mirroring observations from previous studies on ortho-alloy without copper [20]. Consequently, further investigations were conducted using samples fabricated at a substrate preheating temperature of $850 \text{ }^\circ\text{C}$.

In Fig. 3, microstructure images of ortho-alloy samples featuring varying copper content are presented. Irrespective of the quantity of copper incorporated into the alloy, the samples exhibit a two-phase $\text{B2}/\beta + \text{Ti}_2\text{AlNb}$ microstructure, consistent with X-ray phase analysis findings (Fig. 4). Additionally, X-ray phase analysis indicates a minor presence of the $\alpha_2\text{-Ti}_3\text{Al}$ phase (white color), with its abundance increasing alongside the copper content in the alloy. However, specific Ti_2Cu intermetallic precipitates, typical in the Ti–Cu system, were not observed in the microstructure of the fabricated samples. This absence might be attributed to the high cooling rate inherent in the SLM process. A notable characteristic of the resulting microstructures is the influence of the melt bath outlines. The boundaries of the melt baths primarily exhibit small equiaxed grains, while elongated grains are predominantly observed in the center of the bath (Fig. 3, *c*). This distribution pattern mirrors the direction of heat dissipation, which largely coincides with the growth direction. For example, the article [27] refers to the formation of a composite microstructure featuring columnar and equiaxed crystallites, positioned differently along the laser movement direction based on scanning speed variations.

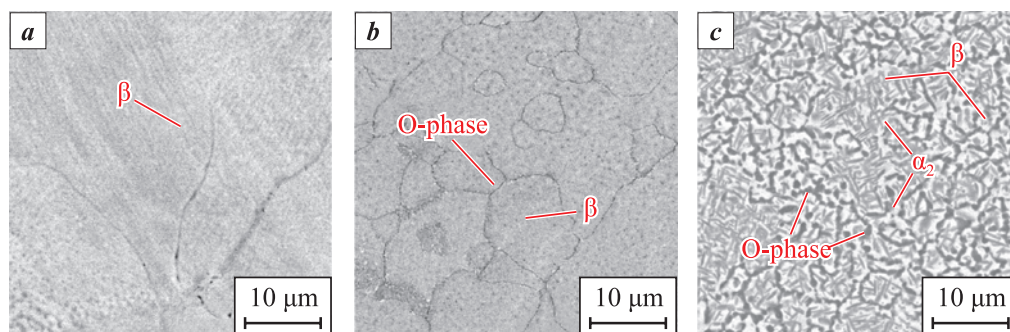


Fig. 2. Microstructure of ortho-alloy with 6 wt. % Cu substrate preheating at $300 \text{ }^\circ\text{C}$ (*a*), $500 \text{ }^\circ\text{C}$ (*b*) and $850 \text{ }^\circ\text{C}$ (*c*)

Рис. 2. Микроструктура орто-сплава с добавлением 6 мас. % меди, изготовленного при температурах подогрева подложки $300 \text{ }^\circ\text{C}$ (*a*), $500 \text{ }^\circ\text{C}$ (*b*) и $850 \text{ }^\circ\text{C}$ (*c*)

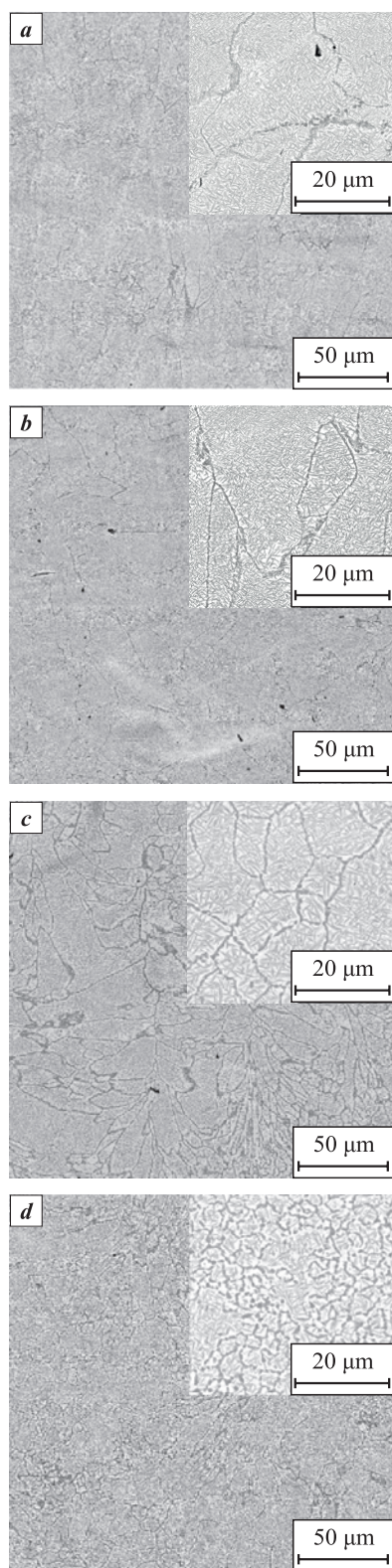


Fig. 3. Microstructure images of ortho-alloy samples produced by SLM, Cu content in the powder mixture Cu, wt. %: *a* – 0; *b* – 2; *c* – 4; *d* – 6

Рис. 3. Изображения микроструктур образцов орто-сплава, изготовленных методом СЛП, при различном содержании меди в порошковой смеси Cu, мас. %: *a* – 0; *b* – 2; *c* – 4; *d* – 6

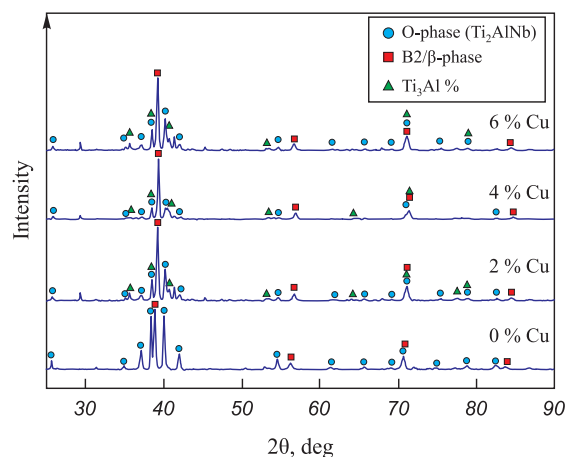


Fig. 4. X-ray phase analysis of ortho-alloy samples with copper content variation produced by SLM method at substrate preheating of 850 °C

Рис. 4. Результаты рентгенофазового анализа образцов орто-сплава с различным содержанием меди, изготовленных методом СЛП при температуре подгрева подложки 850 °C

Fig. 5 presents the results obtained from the differential scanning calorimetry (DSC) analysis conducted on $\text{Ti}_{22}\text{Al}_{25}\text{Nb}$ alloys, both with the inclusion of 6 wt. % copper and without it. In both cases, an exothermic transformation within the temperature range of $t = 631 \div 663$ °C is observed during preheating, linked to the precipitation of the orthorhombic phase. Furthermore, the curve exhibits an inflection towards the endothermic transformation within the B2/β + O zone, potentially correlated with the eutectoid decomposition of B2/β, leading to the formation of $\alpha + \text{Ti}_2\text{Cu}$. The DSC curve for the copper-doped alloy displays a noticeable shift in the peaks of phase transformations, expanding the regions associated with O-Ti₂AlNb and B2/β + O. Consequently, this narrows the region wherein the α_2 -Ti₃Al intermetallic compound is formed. However, it's important to note that doping with copper did not significantly impact the temperature associated with the O + B2/β → B2 phase transition.

The incorporation of copper into the ortho-alloy via *in situ* doping during the SLM process, conducted under substrate preheating conditions at $t = 850$ °C, notably facilitated significant grain refinement. A clear trend toward grain size reduction is observed, commencing with the addition of 2 wt. % Cu, resulting in almost a halving of the β-phase grain size (Fig. 6). The average grain size in the ortho-alloy lacking copper addition measured 50.7 μm. Notably, the most substantial grain refinement, achieving an average size of 8.3 μm, was attained with the highest copper content of 6 wt. %. The enhanced thermal conductivity of copper compared to titanium ortho-alloy plays a crucial role in intensifying heat dissipation during melt crystallization in

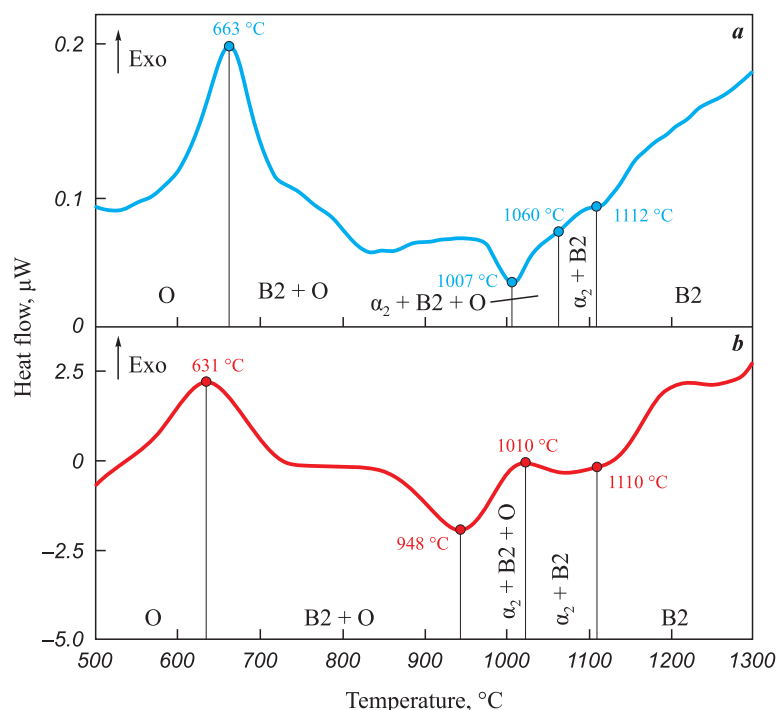


Fig. 5. Results of differential scanning calorimetry of ortho-alloy samples with 6 % copper (a) and without copper (b) produced by SLM at substrate preheating of 850 °C

Рис. 5. Результаты дифференциальной сканирующей калориметрии образцов орто-сплава с содержанием меди 6 % (a) и без меди (b), изготовленных методом СЛП при температуре подогрева подложки 850 °C

the laser processing, consequently promoting the formation of a finer-grained microstructure [13]. Additionally, the presence of copper particles can induce the formation of secondary phases that effectively impede grain growth [10].

Fig. 7 illustrates the tensile curves of ortho-alloy samples containing varying copper content. The alteration in the mechanical properties of the alloy showcases a complex trend, where an increase in copper content initially results in heightened strength, particularly evident with 2 wt. % Cu. However, further escalation of copper

content leads to a reduction in strength and eventual embrittlement of the alloy, despite the reduction in grain size. This embrittlement might be attributed to the formation and enlargement of brittle precipitates, particularly the intermetallic O-phase, located along the grain boundaries [16; 24]. It's worth noting that the tensile strength exhibited by the ortho-alloy containing 2 wt. % Cu in its initial state following SLM is compa-

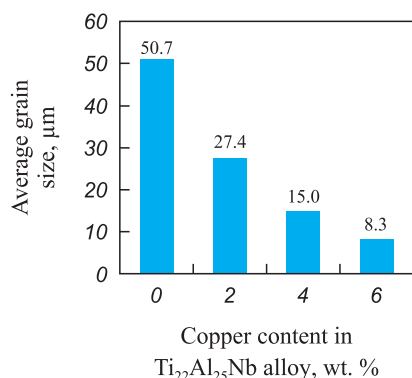


Fig. 6. Average grain size of ortho-alloy produced by SLM with different copper content

Рис. 6. Средний размер зерна орто-сплава, изготовленного методом СЛП, при различном содержании меди

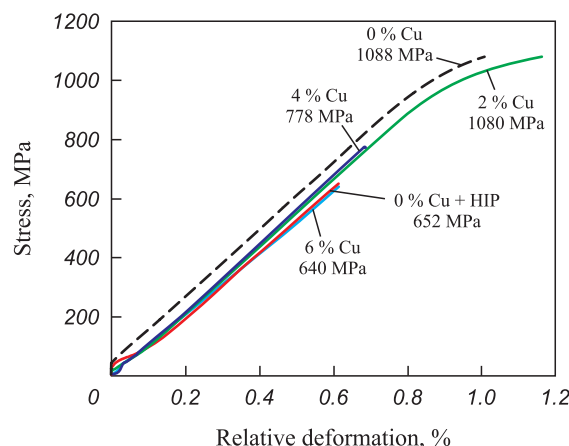


Fig. 7. Room temperature tensile test results for ortho-alloy samples with varying copper content

Рис. 7. Результаты испытаний на растяжение при комнатной температуре для образцов орто-сплава с различным содержанием меди

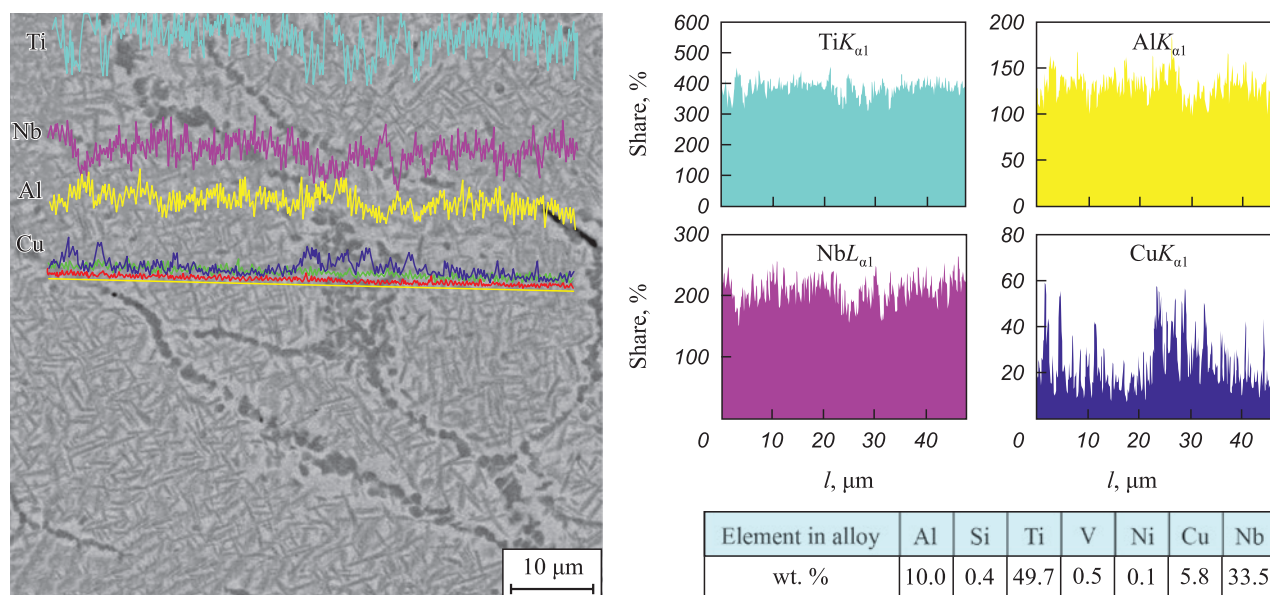


Fig. 8. Energy dispersive analysis of ortho-alloy sample with 6 wt. % Cu

Рис. 8. Результаты энергодисперсионного анализа образца орто-сплава с 6 мас. % меди

table in value to the strength of the ortho-alloy lacking copper, obtained via the SLM method followed by hot isostatic pressing and subsequent heat treatment [17].

The hardness of ortho-alloy samples displays an uneven change with increasing copper content. Incorporating 2 wt. % Cu into the ortho-alloy resulted in a 5 % increase in hardness, measuring 388 HV_{0.5} compared to the sample without copper. Subsequently, the highest microhardness values of 405 HV_{0.5} were achieved with a copper content of 6 wt. %, corresponding to the smallest grain size and a higher quantity of the intermetallic phase. The initial hardness of the ortho-alloy lacking copper stood at 360 HV_{0.5}. Therefore, the addition of 6 wt. % Cu led to a 12 % increase in hardness. The observed higher hardness values are attributed to the refined grains brought about by the addition of copper, leading to a higher density of grain boundaries where the orthorhombic intermetallic phase precipitates form. Notably, an optimal ratio between α_2 -Ti₃Al and the ortho-phase, found in the alloy containing 4 wt. % Cu, resulted in a hardness of 364 HV_{0.5}.

However, the addition of 4 wt. % Cu, despite grain refinement, led to the embrittlement of the alloy. This effect is observed in conditions of high concentration of grain boundaries where a fringe of a brittle intermetallic phase exists. EDX analysis (Fig. 8) indicated a higher concentration of titanium, aluminum, and copper on the grain boundaries compared to the main grain volume. To mitigate the quantity of embrittlement phases along the grain boundaries, additional heat treatment may be considered, which will be explored in future research articles.

Conclusions

This study investigates the impact of copper on the microstructure and mechanical properties of an orthorhombic titanium alloy manufactured through *in situ* doping during the selective laser melting process. The study's key conclusions are as follows:

1. Introduction of copper (0 to 6 wt. %) results in a significant microstructure refinement, yielding fine equiaxed grains. Within the studied copper content range, the phase composition of the ortho-alloy primarily consists of a two-phase B2/β + Ti₂AlNb microstructure, with a limited presence of α_2 -Ti₃Al phase.

2. Variation in substrate preheating temperatures during the SLM process (ranging from 300 to 850 °C) leads to distinct alterations in the alloy's microstructure and phase composition. Starting with a singular B2/β-phase at 300 °C, the process progresses to the formation of the O-phase, accompanied by the precipitation of the Ti₃Al phase at a substrate preheating temperature of 850 °C. Notably, high-temperature substrate preheating serves as an effective method to prevent crack formation during the SLM process.

3. The addition of 6 wt. % Cu resulted in a 12 % increase in the hardness of the ortho-alloy compared to the alloy without copper. However, the inclusion of 4 wt. % Cu notably enhanced the alloy's strength, achieving a tensile strength of 1080 MPa, which is comparable to the strength of the copper-free ortho-alloy produced using SLM technology followed by hot isostatic pressing.

4. Embrittlement observed in the orthorhombic intermetallic alloy could be attributed to the suppres-

sion of the ortho phase, leading to its precipitation along grain boundaries and subsequent decay. This phenomenon is exacerbated by grain refinement induced by the presence of copper in the alloy.

References / Список литературы


1. Illarionov A.G., Stepanov S.I., Naschetnikova I.A., Popov A.A., Soundappan P., Thulasi Raman K.H., Suwas S. A review – additive manufacturing of intermetallic alloys based on orthorhombic titanium aluminide Ti_2AlNb . *Materials*. 2023;16(3):991. <https://doi.org/10.3390/ma16030991>
2. Zhang H., Yang M., Xu Y., Sun C., Chen G., Han F. Constitutive behavior and hot workability of a hot isostatic pressed Ti–22Al–25Nb alloy during hot compression. *Journal of Materials Engineering and Performance*. 2019;28(11):6816–6826. <https://doi.org/10.1007/S11665-019-04453-W/FIGURES/12>
3. Novak A.V., Alekseev E.B., Ivanov V.I., Dzunovich D.A. The study of the quenching parameters influence on structure and hardness of orthorhombic titanium aluminide alloy VTI-4. *Trudy VIAM*. 2018;2(62):5. (In Russ.).
 Новак А.В., Алексеев Е.Б., Иванов В.И., Дзунович Д.А. Изучение влияния параметров закалки на структуру и твердость интерметаллидного титанового орто-сплава ВТИ-4. *Труды ВИАМ*. 2018;2(62):5. <https://doi.org/10.18577/2307-6046-2018-0-2-5-5>
4. Yang J.L., Wang G.F., Zhang W.C., Chen W.Z., Jiao X.Y., Zhang K.F. Microstructure evolution and mechanical properties of P/M Ti–22Al–25Nb alloy during hot extrusion. *Materials Science and Engineering: A*. 2017;699:210–216. <https://doi.org/10.1016/j.msea.2017.05.019>
5. Raji S.A., Popoola A.P.I., Pityana S.L., Popoola O.M. Characteristic effects of alloying elements on β solidifying titanium aluminides: A review. *Heliyon*. 2020;6(7):e04463. <https://doi.org/10.1016/j.heliyon.2020.e04463>
6. Duan B., Yang Y., He S., Feng Q., Mao L., Zhang X., Jiao L., Lu X., Chen G., Li C. History and development of γ -TiAl alloys and the effect of alloying elements on their phase transformations. *Journal of Alloys and Compounds*. 2022;909:164811. <https://doi.org/10.1016/J.JALLCOM.2022.164811>
7. Hussain M.Z., Jiangtao X., Jinglong L., Siddique F., Zhang L.J., Zhou X.R. Effect of Ta microalloying on joint performance by tailoring the microstructure during laser beam welding of Ti–22Al–27Nb. *Materials Science and Engineering: A*. 2022;845:143157. <https://doi.org/10.1016/j.msea.2022.143157>
8. Yang X., Zhang B., Bai Q., Xie G. Correlation of microstructure and mechanical properties of Ti_2AlNb manufactured by SLM and heat treatment. *Intermetallics*. 2021;139:107367. <https://doi.org/10.1016/J.INTERMET.2021.107367>
9. Akbarpour M.R., Mirabad H.M., Hemmati A., Kim H.S. Processing and microstructure of Ti–Cu binary alloys: A comprehensive review. *Progress in Materials Science*. 2022;127:100933. <https://doi.org/10.1016/j.pmatsci.2022.100933>
10. Cardoso F.F., Cremasco A., Contieri R.J., Lopes E.S.N., Afonso C.R.M., Caram R. Hexagonal martensite decomposition and phase precipitation in Ti–Cu alloys. *Materials & Design*. 2011;32(8–9):4608–4613. <https://doi.org/10.1016/j.matdes.2011.03.040>
11. Zhang D., Qiu D., Gibson M.A., Zheng Y., Fraser H.L., StJohn D.H., Easton M.A. Additive manufacturing of ultrafine-grained high-strength titanium alloys. *Nature*. 2019;576(7785):91–95. <https://doi.org/10.1038/s41586-019-1783-1>
12. Donthula H., Vishwanadh B., Alam T., Borkar T., Contieri R.J., Caram R., Banerjee R., Tewari R., Dey G.K., Banerjee S. Morphological evolution of transformation products and eutectoid transformation(s) in a hyper-eutectoid Ti–12 at.% Cu alloy. *Acta Materialia*. 2019;168:63–75. <https://doi.org/10.1016/j.actamat.2019.01.044>
13. Popovich A.A., Sufiarov V.S., Polozov I.A., Grigoriev A.V. Selective laser melting of the intermetallic titanium alloy. *Russian Journal of Non-Ferrous Metals*. 2019;60(2):186–193. <https://doi.org/10.3103/S1067821219020081>
14. Leder M.O., Kondrashov E.N., Rusakov K.A., Dolmato E.V., Maslov N.V., Shchetnikov N.V. Liquefaction defects in ortho-alloys VTI-4 and VIT1. In: *Modern achievements in the field of creating promising light alloys and coatings for aviation and space technology*. Collection of reports of the All-Russian scientific and technical conference (Moscow, 16 April 2021). Moscow: All-Russian Research Institute of Aviation Materials, 2021. P. 159–170. (In Russ.).
 Ледер М.О., Кондрашов Е.Н., Русаков К.А., Долматов Е.В., Маслов Н.В., Щетников Н.В. Ликвационные дефекты в орто-сплавах ВТИ-4 и ВИТ1. В сб.: *Современные достижения в области создания перспективных легких сплавов и покрытий для авиационной и космической техники*. Сборник докладов Всеросс. науч.-техн. конф. (Москва, 16 апр. 2021 г.). М.: Всероссийский научно-исследовательский институт авиационных материалов, 2021. С. 159–170.
15. Cobbinah P.V., Matizamhuka W.R. Solid-state processing route, mechanical behaviour, and oxidation resistance of TiAl alloys. *Advances in Materials Science and Engineering*. 2019;2019:ID4251953. <https://doi.org/10.1155/2019/4251953>
16. Zhang P., Zeng W., Zhang F., Ma H., Xu J., Liang X., Zhao Y. Fracture toughness of Ti_2AlNb alloy with different Al content: Intrinsic mechanism, extrinsic mechanism and prediction model. *Journal of Alloys and Compounds*. 2023;952:170068. <https://doi.org/10.1016/j.jallcom.2023.170068>
17. Wang J., Luo Q., Wang H., Wu Y., Cheng X., Tang H. Microstructure characteristics and failure mechanisms of Ti–48Al–2Nb–2Cr titanium aluminide intermetallic alloy fabricated by directed energy deposition technique. *Additive Manufacturing*. 2020;32:101007. <https://doi.org/10.1016/j.addma.2019.101007>
18. Li Z., Chang B., Cui Y., Zhang H., Liang Z., Liu C., Wang L., Du D., Chang S. Effect of twin-wire feeding methods on the in-situ synthesis of electron beam fabricated Ti–Al–Nb intermetallics. *Materials & Design*. 2022;215:110509. <https://doi.org/10.1016/J.MATDES.2022.110509>
19. Yang X., Zhang B., Bai Q., Xie G. Correlation of microstructure and mechanical properties of Ti_2AlNb manufactured by

- SLM and heat treatment. *Intermetallics*. 2021;139: 107367. <https://doi.org/10.1016/J.INTERMET.2021.107367>
20. Polozov I., Gracheva A., Popovich A. Processing, microstructure, and mechanical properties of laser additive manufactured Ti₂AlNb-based alloy with carbon, boron, and yttrium microalloying. *Metals*. 2022;12(8):1304. <https://doi.org/10.3390/met12081304>
 21. Wang Q., Zhang K., Niu W. Microstructural characteristic and mechanical properties of titanium-copper alloys *in-situ* fabricated by selective laser melting. *Journal of Alloys and Compounds*. 2021;885:161032. <https://doi.org/10.1016/j.jallcom.2021.161032>
 22. Wang Guofeng, Yang Jianlei, Jiao Xueyan. Microstructure and mechanical properties of Ti–22Al–25Nb alloy fabricated by elemental powder metallurgy. *Materials Science and Engineering: A*. 2016;654:69–76. <https://doi.org/10.1016/j.msea.2015.12.037>
 23. Sim Kyong Ho, Wang Guofeng, Kim Tae Jong, Ju Kyong Sik. Fabrication of a high strength and ductility Ti–22Al–25Nb alloy from high energy ball-milled powder by spark plasma sintering. *Journal of Alloys and Compounds*. 2018;741:1112–1120. <https://doi.org/10.1016/J.JALLCOM.2018.01.279>
 24. Kanyane L.R., Popoola A.P., Pityana S., Tlotleng M. Heat-treatment effect on anti-corrosion behaviour and tribological properties of LENS *in-situ* synthesized titanium aluminide. *International Journal of Lightweight Materials and Manufacture*. 2022;5(2):153–161. <https://doi.org/10.1016/J.IJLMM.2021.11.006>
 25. Vilardell A.M., Yadroitsev I., Yadroitsava I., Albu M., Takata N., Kobashi M., Krakhmalev P., Kouprianoff D., Kothleitner G., Plessis A.du. Manufacturing and characterization of *in-situ* alloyed Ti6Al4V(ELI)–3at.%Cu by laser powder bed fusion. *Additive Manufacturing*. 2020;36: 101436. <https://doi.org/10.1016/j.addma.2020.101436>
 26. Polozov I., Sufiarov V., Kantyukov A., Razumov N., Goncharov I., Makhmutov T., Silin A., Kim A., Starikov K., Shamshurin A. Microstructure, densification, and mechanical properties of titanium intermetallic alloy manufactured by laser powder bed fusion additive manufacturing with high-temperature preheating using gas atomized and mechanically alloyed plasma spheroidized powder. *Additive Manufacturing*. 2020;34:101374. <https://doi.org/10.1016/J.ADDMA.2020.101374>
 27. Zhou Y.H., Li W.P., Zhang L., Zhou S.Y., Jia X., Wang D.W., Yan M. Selective laser melting of Ti–22Al–25Nb intermetallic: Significant effects of hatch distance on microstructural features and mechanical properties. *Journal of Materials Processing Technology*. 2020;276:116398. <https://doi.org/10.1016/j.jmatprotec.2019.116398>

Information about the Authors




Igor A. Polozov – Cand. Sci. (Eng.), Assistant Professor, Peter the Great St. Petersburg Polytechnic University (SPbPU)

 **ORCID:** 0000-0002-5380-3072


 **E-mail:** polozov_ia@spbstu.ru

Viktoria V. Sokolova – Engineer, Postgraduate Student, SPbPU

 **ORCID:** 0009-0008-8279-2617


 **E-mail:** sokolova.vero@ya.ru

Anna M. Gracheva – Engineer, Student, SPbPU

 **ORCID:** 0009-0003-2567-3332

 **E-mail:** gracheva.am@mail.ru

Anatoly A. Popovich – Dr. Sci. (Eng.), Professor, Director of the Institute of Machinery, Materials and Transport, SPbPU

 **ORCID:** 0000-0002-5974-6654

 **E-mail:** popovicha@mail.ru

Сведения об авторах

Игорь Анатольевич Полозов – к.т.н., доцент, Санкт-Петербургский политехнический университет Петра Великого (СПбПУ)

 **ORCID:** 0000-0002-5380-3072


 **E-mail:** polozov_ia@spbstu.ru

Виктория Владиславовна Соколова – инженер, аспирант СПбПУ

 **ORCID:** 0009-0008-8279-2617

 **E-mail:** sokolova.vero@ya.ru

Анна Максимовна Грачева – инженер, студент СПбПУ

 **ORCID:** 0009-0003-2567-3332

 **E-mail:** gracheva.am@mail.ru

Анатолий Анатольевич Попович – д.т.н., проф., директор Института машиностроения, материалов и транспорта СПбПУ

 **ORCID:** 0000-0002-5974-6654

 **E-mail:** popovicha@mail.ru

Contribution of the Authors



I. A. Polozov – determined the purpose of the work, conducted the experiments, and wrote the article.

V. V. Sokolova – wrote the article, participated in the discussion of the results.

A. M. Gracheva – prepared initial mixtures, conducted metallographic and X-ray phase analysis, took part in the discussion of the results.

A. A. Popovich – participated in the discussion of the results, determined the purpose of the work.

Вклад авторов

И. А. Полозов – определение цели работы, проведение экспериментов, написание статьи.

В. В. Соколова – написание статьи, участие в обсуждении результатов.

А. М. Грачева – подготовка исходных смесей, проведение металлографического и рентгенофазового анализов, участие в обсуждении результатов.

А. А. Попович – участие в обсуждении результатов, определение цели работы.

Received 23.06.2023

Revised 31.07.2023

Accepted 03.08.2023

Статья поступила 23.06.2023 г.

Доработана 31.07.2023 г.

Принята к публикации 03.08.2023 г.